UDK   519.718:661.887

Thermal Diffusivity of Single Crystal $Bi_{0.9}Sb_{0.1}$

P. M. Nikolić[1*)], S. S. Vujatović[1], T. Ivetić[1], M. V. Nikolić[2], O. Cvetković[3], O. S. Aleksić[2], V. Blagojević[4], G. Brankovic[2], N. Nikolić[2]

[1]Institute of Technical Sciences of SASA, Knez Mihailova 35/IV, 11000 Belgrade, Republic of Serbia
[2]Institute for Multidisciplinary Research, Kneza Višeslava 1, 11000 Belgrade, Republic of Serbia
[3]IchTM, Center of Chemistry, Studentski Trg 12, 11000 Belgrade, Republic of Serbia
[4]Faculty of Electrical Engineering, University of Belgrade, Bulevar Kralja Aleksandra 73, 11000 Belgrade, Republic of Serbia

Abstract:

A single crystal $Bi_{0.9}Sb_{0.1}$ ingot was synthesized using the Bridgman technique. Thermal diffusivity and electronic transport properties of single crystal cleaved plates (00l) were determined from PA photoacoustic phase and amplitude spectra obtained using the photoacoustic method with a transmission detection configuration. Both the PA phase and amplitude were measured versus the modulation frequency and numerically analyzed. EDS analyses done to determine chemical composition of the studied samples as well as to check sample homogeneity. Hall effect measurements data were used for the photoacustic measurements.

Keywords: *Photoacoustic spectroscopy, $Bi_{0.9}Sb_{0.1}$, Thermal diffusivity*

Introduction

It is well known that semiconductors with a relatively small band gap exhibit very good thermoelectric performance. Semi-metallic materials can be made semiconducting by using low dimensionality quantum confinement effects. BiSb alloys are very interesting for thermoelectric applications. Thermoelectric transport properties of doped $Bi_{0.91}Sb_{0.09}$ thin films were examined a long time ago [1, 2]. When Bi-Sb alloys were doped with Pb or Sn the Seebeck coefficient and power factor increased [3]. A photo-thermoelectrical YBCO-BiSb thick film bolometer [4] has been made and used and also BiSb thermocouple sensors in the 8 mm wave length range [5].

2. Experimental and Results

Pure Bismuth (3N) and Antimony (6N) were synthesized using the Bridgman technique at the maximum temperature of about 500ºC. The temperature gradient was 2ºC/mm in the zone of heating and 5ºC/mm in the zone of cooling. The ingot was grown at the speed of 12 mm/h. Using the X-ray technique, the sample composition was confirmed.

---

*) Corresponding author: pantelija.nikolic@sanu.ac.rs

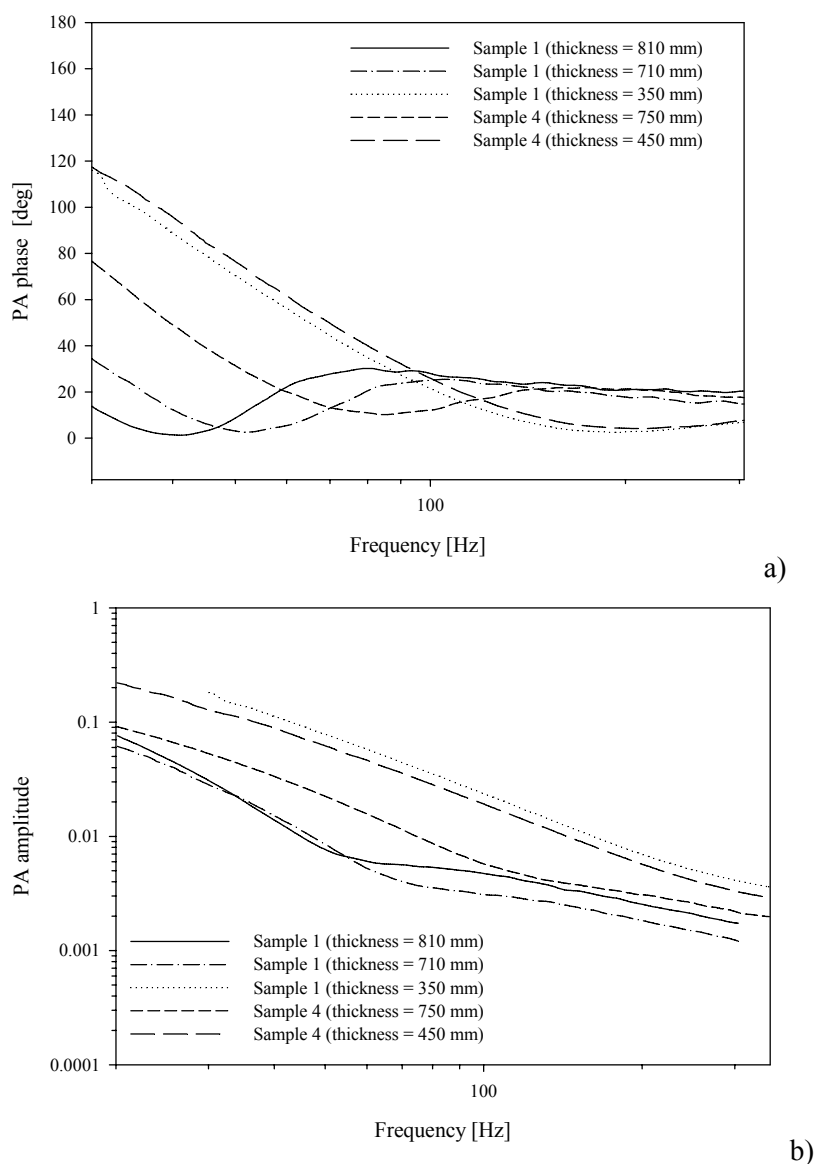Single crystal plates were cleaved, from the ingot, and Bragg's diffractions confirmed its orientation (00l).

a)

b)

Fig. 1 - PA phase (a) and amplitude (b) spectra versus the modulation frequency for $Bi_{0.9}Sb_{0.1}$ sample 1 and sample 4 of different thicknesses and compositions having 12.21 at% Sb and 0.45 at% Sb

Two cleaved thick crystal plates were selected for further measurements – sample 1 and sample 4 of the initial thicknesses of 810 μm and 750 μm, respectively. The chemical composition of two cleaved plates were determined using an Oxford Instruments INCA Penta FETX3 energy dispersive spectrometer (EDS) system attached to a TESCAN Electron Microscope VEGA TS 5130MM scanning electron microscope (SEM). The back-scatter imaging revealed relatively large scale homogeneity of both samples. Bi and Sb contents of sample 1 are 87.79±0.53 at% and 12.21±0.53 at%, respectively. Bi and Sb contents of sample 4 are 99.55±0.10 at% and 0.45±0.10 at%, respectively.

PA amplitude and phase spectra were measured using a specially constructed PA cell [6] whose construction was optimized to obtained maximal acoustical protection from the

surrounding influences. Thus a favorable signal-noise ratio and a flat frequency characteristic were achieved in the range between 60 and 6000 Hz. The PA signals were measured using an experimental setup with a red laser (80 mW) as the optical source. The laser beam was modulated by a mechanical chopper and the sample was irradiated by a large spot (3 mm in diameter) in order to exclude the effect of lateral diffusion in the sample being studied. The sample was mounted directly on the front of an electret microphone, which had a 2.5 mm diameter circular window as the sound inlet. The amplitude and phase of the PA signals for both sample 1 and sample 4 were measured for different plate thicknesses (sample 1 for the initial thickness of 810 μm, repolished to 710 μm and measured, further repolished to 350 μm and measured again; sample 4 for the initial thickness of 750 μm and repolished to 450 μm and measured again). The amplitude and phase of the PA signals, versus the modulation frequency, for both samples are illustrated in Fig. 1 (a) and (b), respectively. These different thicknesses were obtained by polishing one side of the thick plate with diamond paste.

Hall effect measurements were conducted using the Hall Effect Measurement System Ecopia HMS-3000 at the Faculty of Technical Sciences, Novi Sad. The samples used for measurements were prepared to be in the form of a thin plate or thin disc cut perpendicular to the long axis of a single crystal ingot. All samples were carefully inspected for cavities and scratches and polished if necessary. All measurements were carried out at room temperature (T =300 K) and in a dark chamber in order to avoid excitation of the narrow-gap semiconductor by daily light, that is, to minimize the photoconductive and photovoltaic effects. The source of magnetic field applied perpendicular to the Hall element was a permanent magnet of 0.37 T. I-U and I-R characteristics measurements were performed in 10 steps by varying the applied electric current intensity of ±100 μA, ±500 μA and ±1 mA for each sample. Each sample was measured with different orientation with respect to the four ohmic contacts placed on the periphery of the sample, where possible. In addition, some samples were measured on other side as well. These were done in order to check sample homogeneity and data reproducibility. Hall effect measurements were done to obtain transport properties, that is, mobility of the charge carriers necessary as the entry parameter for the fitting procedure of the photoacoustic measurements. The concentration of the carriers and the mobility of the charge carriers for the studied samples are given in Tab. I.

Tab. I - Parameters obtained by the Hall effect measurements of studied samples

Sample	μ [m^2/Vs]
Sample1	0.2434
Sample 4	0.0314

3. Discussion

In accordance with the Rosencwaig-Gersho thermal pistons model [7] a complex system at the gas-sample-backing-microphone detection configuration is considered. The temperature distribution in the PA cell must be known for determining the amplitude and phase of a PA signal. One should take into account different thermodiffusion mechanisms in thermal wave generation e.g. many thermal sources in semiconductors. Finally that theoretical model shows that the periodic variation of the surface temperature and consequently the PA signal has a complex dependence on the modulation frequency [6, 8]. Since, there is a decrease in the electret microphone sensitivity in the frequency range below about 100 Hz, the experimental amplitude and phase PA signal should be corrected in the modulation

frequency range below 100 Hz. In this work we have used a simple method of normalization PA experimental diagrams of the same sample but with two different thicknesses. This normalization method can eliminate the effect of the electret microphone. The signal ratio for two different thicknesses of the measured sample was calculated using the following equation:

$$\frac{S_1(\omega)}{S_2(\omega)} = \left|\frac{\Phi(-l_1)}{\Phi(-l_2)}\right| e^{[j/\varphi_1(-l_1) - \varphi_2(-l_2)]} = A_m e^{j\Delta\varphi} \tag{1}$$

where $\Phi(-l)$ is temperature distribution on the surface which is in contact with the electret microphone and A_m is amplitude ratio while $\Delta\varphi$ is the phase difference of the experimentally measured PA signals for two different sample thicknesses.
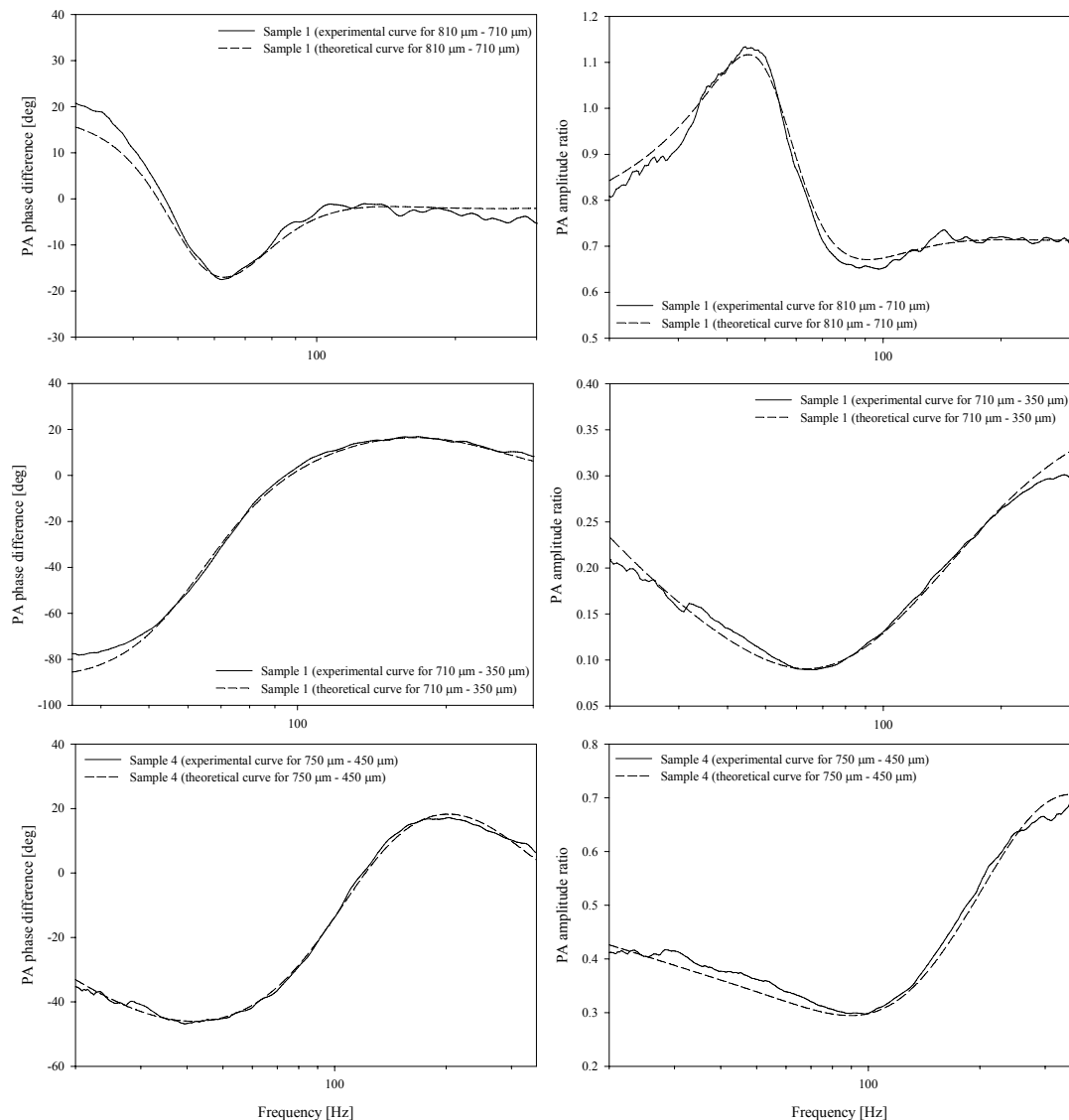

Fig. 2 - PA phase difference and amplitude ratio normalized fitted diagrams for sample 1 and sample 4 of $Bi_{0.9}Sb_{0.1}$ of different thicknesses; experimental data (solid line) and theoretical curve (dashed line).

Typical examples of the amplitude and phase fitted diagrams for both sample 1 and sample 4 of different thicknesses are shown in Fig. 2. The fitting program enables the user to choose the value of parameters existing in the mathematical model. The user can select the magnitude of the change of each parameter. One can simultaneously fit separately the amplitude or phase diagram or both together. In that case the fitting error can be estimated using one of the following criteria: a) the sum of absolute differences between the experimental and the calculated values; b) the sum of the squares of differences between the calculated and the experimental values; c) the sum of relative errors; d) the sum of the squares of the relative errors. Therefore, the experimental curves can be compared with the theoretical one obtained by the mathematical model for the given parameters and their values can be determined during the fitting procedure. Sample 4 shows better fiting due to larger scale homogenity with respect to sample 1, revealed by back-scatter electron imaging.

Tab.II - Parameters obtained by the fitting procedure for two normalized PA spectra of $Bi_{0.9}Sb_{0.1}$

Sample	$D(m^2/s)$	$\tau(\mu s)$	$\alpha(m^{-1})$	$D_T(m^2/s)$
Sample 1 810/710	$2.559 \cdot 10^{-3}$	$2.2 \cdot 10^{-3}$	8817	$0.307 \cdot 10^{-5}$
Sample 1 710/350	$2.559 \cdot 10^{-3}$	$1.4 \cdot 10^{-3}$	7676	$0.308 \cdot 10^{-5}$
Sample 1 710/350	$2.559 \cdot 10^{-3}$	$1.8 \cdot 10^{-2}$	15060	$0.311 \cdot 10^{-5}$
Sample 4 750/450	$2.319 \cdot 10^{-4}$	$6.6 \cdot 10^{-3}$	16206	$0.407 \cdot 10^{-5}$

D was calculated from the mobility of the charge carrier (μ values from Tab. I)
K = 7.8 W/mK in all measurements
The ranges (minimum and maximum values) of the excess carrier lifetime (τ), optical absorption coefficient (α) and thermal diffusivity coefficient (D_T) are given for sample 1 of thickness 810μm/710μm and 710μm/350μm

Tab. II contains the values of the fitted parameters obtained during the fitting procedure for two normalized PA spectra. The values of the following parameters were calculated: excess carrier lifetime (τ), thermal diffusivity coefficient (D_T), rear surface recombination velocity (s_b), front surface recombination velocity (s_g) and optical absorption coefficient (α). The hole diffusion coefficient (D) was calculated from determined mobility of the charge carriers. The maximum and minimum values of the excess carrier lifetime (τ), optical absorption coefficient (α) and thermal diffusivity coefficient (D_T) are determined for sample 1 of thicknesses 810μm/710μm and 710μm/350μm.

It is obvious that the experimental and theoretical diagrams are mainly different in the frequency range below about 40 Hz where the electret microphone sensitivity is limited. At the same time one can notice that the difference between the experimental and theoretical diagrams are small in the frequency range above 40 Hz. Slight discrepancies between experimental and theoretical diagrams are also observed at highest frequencies. That in some way demonstrates that the values of the fitted parameters are reasonably well determined.

Our results can be compared with a limited number of results on the thermal and electrical properties of BiSb alloys. For instance, thermal diffusivity of Bi doped with Sm was measured using the flash technique [9] and the obtained values were between $0.793 \cdot 10^{-6}$ and $0.587 \cdot 10^{-6}$ m^2/s depending on the amount of Sm. Our determined value is higher ($0.3 \cdot 10^{-5}$ to $0.4 \cdot 10^{-5}$ m^2/s), probably due to the presence of Sb in our samples comparing to Sm-doped samples in [9].

4. Conclusion

Single crystal $Bi_{0.9}Sb_{0.1}$ plates with (00l) orientation cleaved from an ingot obtained using the Bridgeman technique were used for PA measurements. The SEM-EDS measurements revealed distinct compositions of the samples 1 and 4 suggesting elemental segregation during crystal growth. Hall effect measurements indicate that $Bi_{0.9}Sb_{0.1}$ alloy is dominantly n-type semiconductor. Using both the amplitude and phase PA spectra for different thickness values of the sample 1 and sample 4, the parameters such as the thermal diffusivity coefficient, hole diffusion coefficient, excess carrier lifetime and optical absorption coefficient were determined.

Acknowledgments

References

1. S. Cho, A. DiVenere, G.K. Wong, J.B. Ketterson, J.R. Meyer, J. Appl. Phys. 85 (1999) 3655-3659.
2. S. Cho, Y. Kim, A. DiVenere, G.K. Wong, J.B. Ketterson, J.R. Meyer, Thermoelectrics Eighteenth International Conference (1999) 205-208.
3. H. Noguchi, H. Kitagawa, T. Kiyabu, K. Hasezaki, Y. Noda, J. Phys. Chem. Solids 68 (2007) 91-95.
4. M.M. Kaila, G.J. Russell, J. Phys. D: Appl. Phys. 31 (1998) 1987-1990.
5. O. Sukhoruchko, A. Tishchenko, Int. J. Infrared and Millimeter Waves 26 (2005) 65-70.
6. P.M. Nikolić, S.S. Vujatović, D.M. Todorović, M.B. Miletić, A. Golubović, A.I. Bojičić, F. Kermendi, S. Djurić, K.T. Radulović, J. Elazar, Jpn. J. Appl. Phys. 36 (1997) 1006-1011.
7. A. Rosencweig, A. Gersho, J. Appl. Phys. 47 (1976) 64-69.
8. D.M. Todorović, P.M. Nikolić, D.M. Dramićanin, D.G. Vasiljević, Z.D. Ristovski, J. Appl. Phys. 78 (1995) 5750-5755.
9. C.L. Teh, Z. A. Wahab, W. M. M. Yunus, M. M. Moksin, S.A. Halim, H. Imad, J. Physics Malaysia 23 (2002) 187-190.

Садржај: Монокристални ингот $Bi_{0.9}Sb_{0.1}$ састава је сиснтетисан Брижмановом техником. Топлотна дифузивност и електронске транспортне особине плочице монокрисатала сечене паралелно плосни (00l) одређене су из фотоакустичних (ПА) спектара амплитуда и фаза применом метода фотоакустике за трансмисиону детекцију. ПА фазе и амплитуде мерене су са променом модулационе фреквенције и нумерички анализиране. Микрохемијском електронском анализом ЕДС методом одређен је хемијски састав и хомогеност узорака. Подаци мерења холовог ефекта коришћени су као полазни параметри за утачњавање фотоакустичних дијаграма.
Кључне речи: Фотоакустична спектроскопија, $Bi_{0.9}Sb_{0.1}$, топлотна дифузивност.